ACCSCIENCE PUBLISHING

International Journal of Bioprinting

RESEARCH ARTICLE

Antibacterial photocurable resin loaded with cetylpyridinium chloride for vat photopolymerization 3D printing in dental applications

Tomoe Nishikawa[1,2], Yuki Nagamatsu[1], Yusaku Nishizawa[1,2], Yasuhiko Akama[1,2], Jun J. Miyamoto[2], Kaori Gunjigake-Kometani[2], Tatsuo Kawamoto[2], and Hiroshi Ikeda[1]*

[1] Division of Biomaterials, Department of Oral Functions, Kyushu Dental University, Fukuoka, Japan

[2] Division of Orofacial Functions and Orthodontics, Department of Health Improvement, Kyushu Dental University, Fukuoka, Japan

Abstract

Bacterial adhesion and biofilm formation are critical issues for 3D-printed dental resin. This study aims to develop a novel cetylpyridinium chloride (CPC)-based antibacterial photocurable resin for vat photopolymerization (VPP) 3D printing and evaluate its printability, mechanical properties, antibacterial activities, and CPC-release behavior for potential use in dental prostheses and orthodontic devices. Photocurable resins containing 0–3 wt.% CPC were formulated from methacrylate and acrylate monomers. Printability of the photocurable resins was assessed by measuring viscosity, cure depth, over-curing, and the degree of conversion. The photocurable resins were printed using a VPP 3D printer, and the resulting specimens were evaluated for mechanical properties using three-point bending and Vickers hardness tests. Antibacterial activity against *Streptococcus mutans* was examined by bacterial viability and plaque-formation assays. CPC-release behavior was analyzed by UV–visible spectroscopy. CPC incorporation up to 3% slightly increased resin viscosity, cure depth, and over-curing while maintaining adequate printability. The degree of conversion was not significantly affected by CPC content. The 1% CPC-loaded printed resin exhibited mechanical properties comparable to the CPC-free control, whereas 3% CPC markedly reduced them. The 1% CPC-loaded resin showed strong antibacterial activity, achieving an antibacterial activity value of 5.6 (>99.99% bacterial reduction), and demonstrated sustained plaque inhibition. Sustained CPC release from the printed resins was confirmed throughout the 14-day evaluation period. These results demonstrate that 1% CPC-loading provides an optimal balance among printability, mechanical properties, and antibacterial performance. The developed material shows potential for application in 3D-printed dental polymer-based prostheses and orthodontic devices.

Keywords: 3D printing; Additive manufacturing; Antibacterials; Biomaterials; Cetylpyridinium chloride; Dental materials; Dental resin

***Corresponding author:**
Hiroshi Ikeda
(r16ikeda@fa.kyu-dent.ac.jp)

Citation: Nishikawa T, Nagamatsu Y, Nishizawa Y, *et al.* Antibacterial photocurable resin loaded with cetylpyridinium chloride for vat photopolymerization 3D printing in dental applications. *Int J Bioprint.* 2026;12(1):607-621. doi: 10.36922/IJB025470484

Received: November 20, 2025
Revised: December 26, 2025
Accepted: January 7, 2026
Published online: January 12, 2026

1. Introduction

Vat photopolymerization (VPP) 3D printing has emerged as a widely adopted additive manufacturing technique for resin-based materials due to its high printing accuracy, excellent surface quality, and cost-effectiveness. In dentistry, VPP systems—including liquid crystal display (LCD), digital light processing, and stereolithography—are increasingly incorporated into digital workflows alongside intraoral optical scanning, computer-aided design (CAD), and computer-aided manufacturing technologies.[1] This comprehensive digital approach enables the precise fabrication of a wide range of dental prostheses and appliances. In particular, VPP-based resin materials have gained notable attention for producing removable orthodontic and prosthodontic devices, such as aligners, retainers, and dentures.[2,3]

Despite these advantages, a major clinical concern associated with VPP-printed resin materials is their high susceptibility to bacterial adhesion and biofilm formation.[4–7] The layer-by-layer fabrication process generates characteristic micro-grooved surface textures, which facilitate microbial retention and biofilm development, thereby increasing the risk of oral diseases such as dental caries and periodontitis.[8] Accordingly, establishing effective strategies to inhibit bacterial colonization on 3D-printed dental resins is essential for improving their long-term clinical performance.

Incorporating antimicrobial agents into dental polymeric materials has been investigated as a promising approach to reduce bacterial adhesion and biofilm formation on prostheses and orthodontic devices. Conventional resin-based dental materials containing antibacterial additives—particularly systems designed for controlled release or surface antibacterial functionalization—have demonstrated significant reductions in microbial colonization.[9,10] Recently, this concept has been extended to dental 3D-printed resins, where antibacterial fillers have been incorporated into the resin matrix to impart antibacterial activity.[11–14] For example, Salgado *et al.*[11] reported that graphene-enhanced printed resin inhibited the growth and biofilm formation of *Candida albicans* and *Streptococcus mutans*. Mangal *et al.*[12] demonstrated that nanodiamond incorporation reduced *S. mutans* adhesion on printed resin surfaces. Jin *et al.*[13] showed that a fluoride-doped resin effectively suppressed *S. mutans* proliferation through sustained fluoride release. Additionally, Khattar *et al.*[14] demonstrated that ZrO_2 incorporation inhibited *C. albicans* adhesion and growth in 3D-printed resins. These advances highlight the potential of antibacterial 3D-printed resins for dental applications.

However, previous studies have not comprehensively examined how incorporating antibacterial agents influences key performance characteristics specific to VPP resin systems—including printability, physicochemical behavior, mechanical integrity, and antibacterial efficacy. These material properties are critical determinants of the clinical success of 3D-printed dental devices. Therefore, a major remaining challenge is to understand how antibacterial additives influence the essential material properties of dental 3D-printed resins that determine their clinical performance.

To develop novel antibacterial photocurable resins for VPP 3D printing, cetylpyridinium chloride (CPC) was selected as the antimicrobial agent. CPC is a quaternary ammonium compound widely used in oral care products, including mouthwashes, denture cleansers, and toothpastes.[15] It exhibits broad-spectrum antibacterial and antifungal activity, along with favorable biocompatibility for intraoral applications. Several studies have investigated CPC-loaded dental polymeric materials and demonstrated their antibacterial performance.[16–25] For example, Namba *et al.*[17] incorporated CPC into methacrylate-based resins, reporting sustained antibacterial activity driven by CPC release into the surrounding environment. Yamamoto *et al.*[26] developed CPC–montmorillonite-loaded resin cement and demonstrated continuous anti-biofilm effects associated with controlled CPC release. However, CPC has not yet been incorporated into photocurable resin matrices used for VPP-based 3D printing in dental applications.

This study aims to develop a CPC-loaded photocurable resin for VPP 3D printing and to evaluate its feasibility for dental applications. A comprehensive assessment was performed, including analyses of printability, mechanical properties, antibacterial activities, and sustained CPC-release behavior of the printed resins.

2. Materials and methods

2.1. Experimental procedure

A schematic overview of the preparation process for CPC-loaded photocurable resins and the subsequent evaluations is shown in Figure 1.

2.2. Fabrication of cetylpyridinium chloride-loaded photocurable resins and vat photopolymerization 3D printing

2.2.1. Preparation of photocurable resin for vat photopolymerization 3D printing

The reagents used to prepare the photocurable resins are listed in Table 1. All procedures were performed at room temperature under ambient laboratory conditions. CPC was first dissolved in 2-hydroxyethyl methacrylate

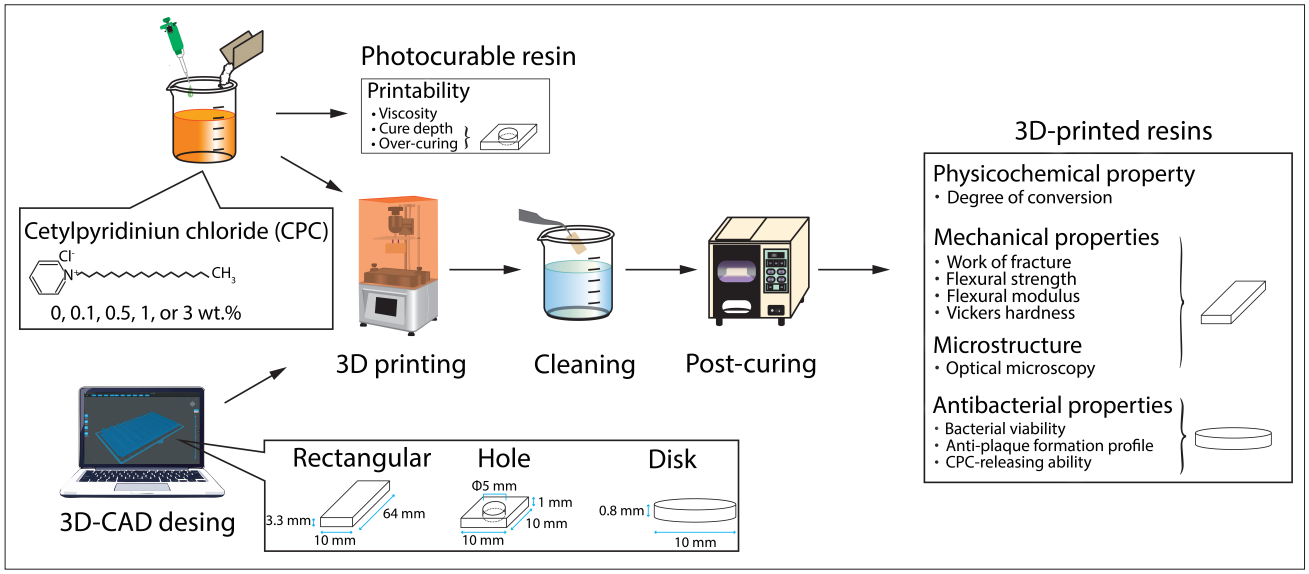

Figure 1. Schematic overview of the fabrication and evaluation workflow for CPC-loaded photocurable resins, highlighting the relationship between resin formulation, vat photopolymerization 3D printing, and subsequent evaluations of printability, mechanical properties, and antibacterial performance. Abbreviation: CAD, computer-aided design; CPC, cetylpyridinium chloride.

(HEMA) by magnetic stirring for 30 min. Separately, the remaining resin components were premixed using a planetary centrifugal mixer (ARE-310, THINKY Corp., Japan) at 2000 rpm for 4 min. The CPC-containing HEMA was then added to the premixed resin and mixed for an additional 2 min. Subsequently, the photo-initiator and photo-absorber were incorporated into the mixture and mixed for another 2 min, followed by a 1-min defoaming cycle to remove entrapped air. The resultant photocurable resin formulations containing 0, 0.1, 0.5, 1, and 3 wt.% CPC were prepared for subsequent experiments.

2.2.2. Computer-aided design model and slicing for 3D printing

Three geometries (rectangular bars, discs, and hole-pattern specimens, as shown in Figure 1) were designed using 3D CAD software (Tinkercad, Autodesk Inc., USA) and exported as STL files. The STL files were processed with slicer software (CHITUBOX Basic, Version 2.1.0, CBD-Tech, China) to generate layer-by-layer print data suitable for import into the 3D printer.

2.2.3. Vat photopolymerization 3D printing and post-treatment

The printing of the CPC-loaded photocurable resins was performed using an LCD-type VPP printer (ELEGOO Mars 3 Pro, ELEGOO, China) with a layer thickness of 0.05 mm and 5 s light exposure per layer. Printed objects were removed from the build platform and ultrasonically cleaned in isopropyl alcohol for 5 min. Post-curing was performed using a xenon-flash curing unit (Otoflash G171, BEGO, Germany) with two cycles of 2000 flashes

Table 1. Materials used for preparing the CPC-loaded photocurable resins for the vat photopolymerization 3D printing

Abbreviation	Material	Type	Weight (g)	Manufacturer
CPC	Celylpyridinium chloride	Antibacterial agent	0, 0.05, 0.25, 0.5, or 1.5	FUJIFILM Wako Pure Chemical Corp, Japan
HEMA	2-Hydroxyethyl methacrylate	CPC-loaded monomer	5.0	FUJIFILM Wako Pure Chemical Corp, Japan
UDMA	Urethane dimethacrylate	Main monomer	20.0	Sigma-Aldrich Co. LLC, Germany
TEGDMA	Triethyleneglycol dimethacrylate	Diluent monomer	20.0	FUJIFILM Wako Pure Chemical Corp, Japan
TMPTA	Trimethylolpropane triacrylate	Cross-linker	5.0	Tokyo Chemical Industry Co., Ltd., Japan
BAPO	Phenylbis(2,4,6-trimethylbenzoyl) phosphine oxide	Photo-initiator	0.25	Tokyo Chemical Industry Co., Ltd., Japan
TBT	2,5-Bis(5-tert-butyl-2-benzoxazolyl)triophene	Photo-absorber	0.05	Tokyo Chemical Industry Co., Ltd., Japan

under an N_2 atmosphere. The post-cured printed resins were subsequently used for the following evaluations.

2.3. Printability evaluation of cetylpyridinium chloride-loaded photocurable resins for vat photopolymerization 3D printing

2.3.1. Viscosity

Viscosities of the photocurable resins were measured at a shear rate of 10 s^{-1} using a rotational rheometer (MCR 92, Anton Paar GmbH, Austria) equipped with a cone-and-plate geometry at 25°C (n = 5).

2.3.2. Cure depth

The photocurable resins were poured into the printer vat and exposed to light for 5 s. The resulting polymerized films were removed, and their thickness was measured using a digital caliper (CD-15CPX, Mitutoyo Corp., Japan). The measured film thickness was defined as the cure depth of the photocurable resins in the VPP 3D printing process (n = 10).

2.3.3. Over-curing

Dimensional accuracy in the XY direction was evaluated using hole-pattern specimens. The diameter of each printed hole was measured with a digital microscope (VHX-600, Keyence Corp., Japan). Over-curing (overgrowth) was quantified as the difference between the designed hole diameter in the CAD model and the measured diameter of the printed specimen (n = 10).

2.3.4. Degree of conversion

Degree of conversion for the printed resins was determined using Fourier-transform infrared spectroscopy (FTIR; IRSpirit, Shimadzu Corp., Japan). The degree of conversion was calculated from the peak intensities at 1638 cm^{-1} (C=C stretch) and 1720 cm^{-1} (C=O stretch) in accordance with previous studies,[27] using the following equation:

$$\text{Degree of conversion (\%)} = \left(\frac{[A(C=C)/A(C=O)]_{\text{after polymerization}}}{[A(C=C)/A(C=O)]_{\text{before polymerization}}} \right) \times 100 \quad (1)$$

where A(C=C) and A(C=O) represent the absorbance intensities of the C=C and C=O bonds, respectively (n = 10).

2.4. Mechanical properties

2.4.1. Three-point bending test

The rectangular bar specimens were used for mechanical testing. The three-point bending test was conducted according to ISO 20795-2:2013 (Dentistry—Base Polymers—Part 2: Orthodontic Base Polymers). According to ISO 20795-2, flexural properties of dental polymer-based materials are evaluated based on load–deflection data obtained from three-point bending tests, and the corresponding mechanical parameters are derived from these measurements using standard beam theory. Testing was performed using a universal testing machine (AGS-H, Shimadzu Corp., Japan) with a support span of 50 mm and a crosshead speed of 5 mm/min (n = 10). Load–deflection curves were recorded to determine the mechanical properties. The work of fracture W (J/m^2) was calculated using:

$$W = \frac{A}{bh} \quad (2)$$

where A represents the area under the load–deflection curve (N·mm), b is the specimen width (mm), and h is the specimen thickness (mm). The flexural strength σ (MPa) was calculated using the following equation:

$$\sigma = \frac{3FL}{2bh^2} \quad (3)$$

where F is the maximum load (N), and L is the distance between the supports (mm). The flexural modulus E (GPa) was calculated from the initial linear region of the load–deflection curve using the following equation:

$$E = \frac{mL^3}{4bh^3} \quad (4)$$

where m is the slope of the initial linear region of the load–deflection curve (N/mm).

2.4.2. Vickers hardness test

The fractured specimens obtained from the three-point bending tests were used for Vickers hardness measurement (n = 10). Hardness was determined using a microhardness tester (HMV-G21ST, Shimadzu Corp., Japan) under a 200 g load applied for 15 s.

2.5. Optical microscopy

The microstructure of the CPC-loaded printed resin surfaces with different CPC contents (0–3 wt.%) was examined using the digital microscope.

2.6. Antibacterial properties

To evaluate the antibacterial properties of the CPC-loaded printed resins, two types of tests were conducted: the antibacterial activity test and the anti-plaque formation

test. Disc-shaped specimens of the printed resins were used in both tests. All printed specimens were sterilized by UV irradiation for 40 min prior to the antibacterial activity and anti-plaque formation tests. The cariogenic bacterium *S. mutans* NBRC 13955 was used as the test microorganism. The bacteria were precultured in brain–heart infusion (BHI) broth at 37°C for 48 h under aerobic conditions. After centrifugation, the bacterial pellet was washed twice with sterile phosphate-buffered saline (PBS) and resuspended in fresh BHI broth to prepare bacterial suspensions with concentrations of 3×10^4 or 3×10^8 CFU/mL. All antibacterial activity and anti-plaque formation tests were performed in five specimens per group ($n = 5$) under identical experimental conditions.

2.6.1. Antibacterial activity test

Each specimen was immersed in 1.0 mL of *S. mutans* suspension (3×10^4 CFU/mL) and incubated at 37°C for 48 h to allow bacterial attachment to the specimen surface. After incubation, the specimens were transferred to 10 mL of sterile PBS and ultrasonically cleaned for 5 min to detach adherent bacteria. The resulting bacterial suspensions were serially diluted, and 0.2 mL of each dilution was spread onto BHI agar plates. After incubation at 37°C for 48 h, the colonies were counted to determine the number of viable adherent bacteria. To quantitatively compare the antibacterial performance of the CPC-loaded printed resins with that of the CPC-free printed resins, the antibacterial activity value (R) was calculated using the following equation:

$$R = \log_{10} NB_0 - \log_{10} NB_n \quad (5)$$

where NB_0 and NB_n represent the numbers of viable bacteria obtained from specimens containing 0% and n% CPC, respectively ($n = 0.1$, 0.5, 1, or 3).

2.6.2. Anti-plaque formation test

To evaluate the sustained antibacterial activity of the CPC-loaded printed resins, plaque formation before and after CPC release from the specimens was investigated. CPC-free (0%) and 1% CPC-loaded printed resin specimens were used. To induce CPC release, the specimens were immersed in distilled water at 37°C for 14 days. After immersion, the specimens were rinsed with sterile PBS and then incubated in 1.0 mL of *S. mutans* suspension (3×10^8 CFU/mL) at 37°C for 48 h to allow plaque formation. After gentle rinsing with distilled water, the plaque formed on the upper surface area (0.785 cm^2) was stained using a plaque-disclosing agent (DENT Liquid Plaque Tester AR, Lion Dental Products Co., Japan). The stained specimens were photographed using a digital camera (EOS Kiss X7, Canon Inc, Japan), and the images were analyzed with ImageJ2 software (National Institutes of Health, Bethesda, USA). The stained area was quantified using a saturation threshold value of 102 in the hue, saturation, brightness color model. The plaque formation rate (%) was calculated using the following equation:

$$\text{Plaque formation rate}\,(\%) = \frac{\text{Plaque - stained area}}{\text{Total surface area}} \times 100 \quad (6)$$

2.7. Cetylpyridinium chloride-release behavior test

Disc-shaped specimens were immersed individually in 10 mL of distilled water at 37°C and stored for 14 days. The absorbance of the immersion solutions was measured every few days using a UV–visible (Vis) spectrophotometer (V-650S, JASCO Corp., Japan). CPC exhibits a characteristic absorption peak near 260 nm; therefore, a calibration curve was prepared using aqueous solutions of known CPC concentrations. The CPC concentration in each sample was calculated based on the absorbance at 260 nm ($n = 10$).

2.8. Statistical analysis

All data were analyzed using EZR statistical software (Saitama Medical Center, Jichi Medical University, Japan). For multiple group comparisons, one-way analysis of variance followed by Tukey's post-hoc test was performed. For pairwise comparisons, the Student's t-test was used. Statistical significance was set at $p < 0.05$ for all analyses.

3. Results

3.1. Printability of the photocurable resins

The printability of the photocurable resins for VPP 3D printing was evaluated in terms of viscosity, cure depth, over-curing behavior, and degree of conversion.

Figure 2A shows the viscosity of the photocurable resins measured using a rheometer at a shear rate of 10 s^{-1}. This shear rate reflects the resin flow behavior during the VPP process, as it corresponds to the fluidity of the resin in the vat.[28] The viscosity of the CPC-free photocurable resin was 554 ± 41 mPa·s, and it increased with increasing CPC content. The 3% CPC-loaded printed resin exhibited a viscosity of 667 ± 85 mPa·s.

Figure 2B presents the cure depth of the photocurable resins after light exposure in the printer vat. No significant differences in cure depth were observed among the formulations, indicating that CPC incorporation up to 3% did not impair photopolymerization efficiency under the selected exposure conditions.

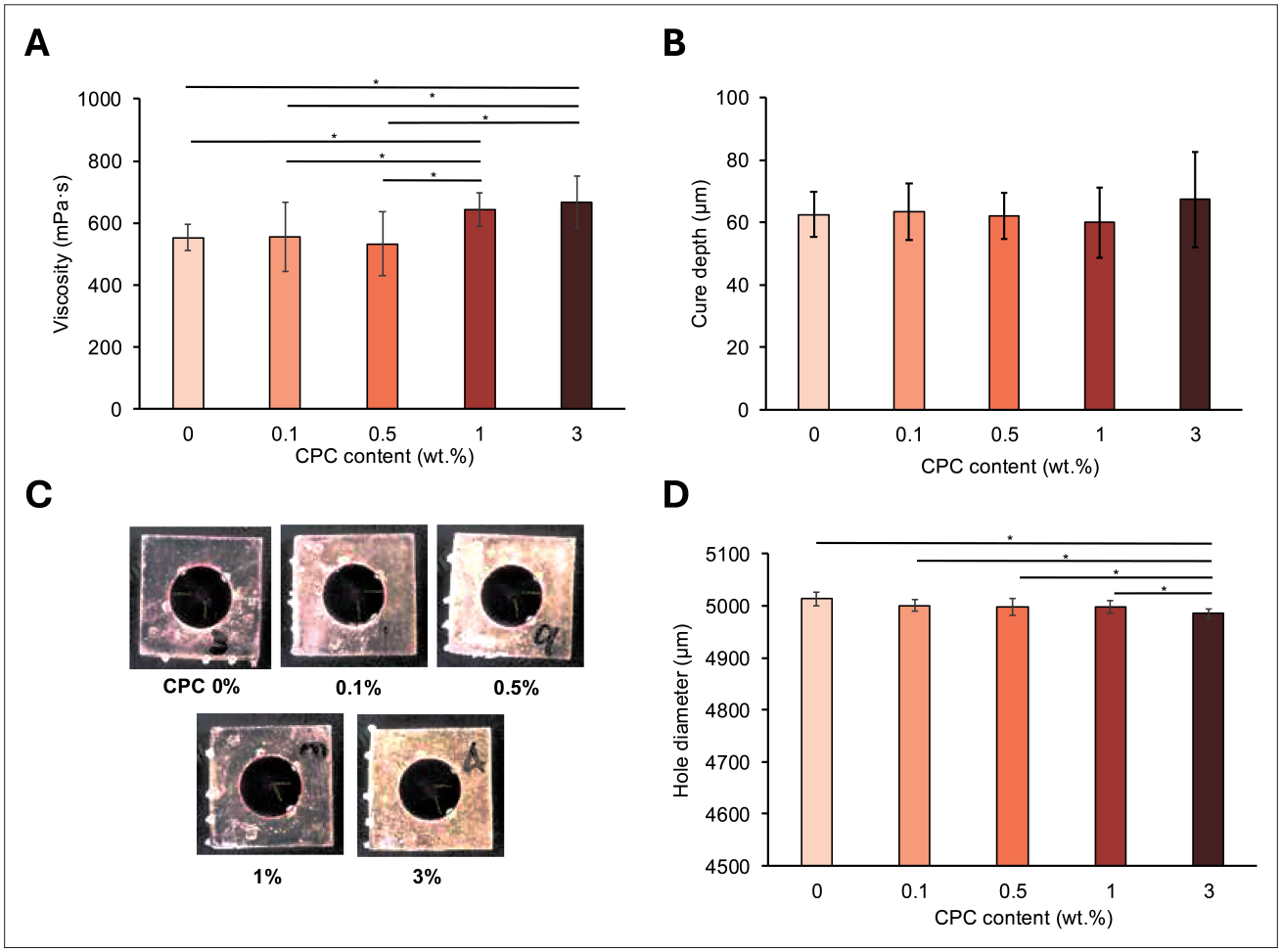

Figure 2. Printability of the photocurable resins for vat photopolymerization (VPP) 3D printing. (A) Viscosity of the photocurable resins with different cetylpyridinium chloride (CPC) contents. (B) Cure depth of the photocurable resins photopolymerized by 5 s of light exposure using the 3D printer. (C) Representative microscope images of the printed specimens with a hole pattern used to evaluate over-curing. (D) Quantification of over-curing calculated from the hole-pattern images shown in (C). These results indicate that CPC incorporation up to 1 wt.% maintains adequate resin flowability, curing behavior, and dimensional accuracy required for stable VPP 3D printing. Note: $*p < 0.05$.

Figure 2C shows representative microscopic images of hole-pattern printed resin specimens fabricated with different CPC concentrations, and Figure 2D quantifies over-curing based on the measured hole diameters. The hole diameter decreased with increasing CPC content. The CPC-free printed resin exhibited a hole diameter of 5013 ± 14 μm, whereas the 3% CPC-loaded printed resin showed a reduced diameter of 4984 ± 10 μm. A decrease in hole diameter indicates a greater degree of over-curing. Therefore, over-curing tended to increase as the CPC concentration increased. However, no significant difference was observed between the 0% and 1% CPC-loaded printed resins, indicating that CPC addition up to 1% does not significantly compromise lateral printing accuracy.

Figure 3 shows the degree of conversion of the printed resins. No significant differences were observed among the groups, indicating that CPC incorporation up to 3% did not adversely affect the polymerization efficiency of the photocurable resin.

3.2. Mechanical properties

The mechanical properties of the CPC-loaded printed resins, including work of fracture, flexural strength, flexural modulus, and Vickers hardness, are shown in Figure 4. The work of fracture, flexural strength, and Vickers hardness decreased with increasing CPC content. In particular, the 3% CPC-loaded printed resin showed significantly lower values compared with the CPC-free printed resin, whereas no significant differences were observed between the 0% and 1% CPC groups. In contrast, the flexural modulus

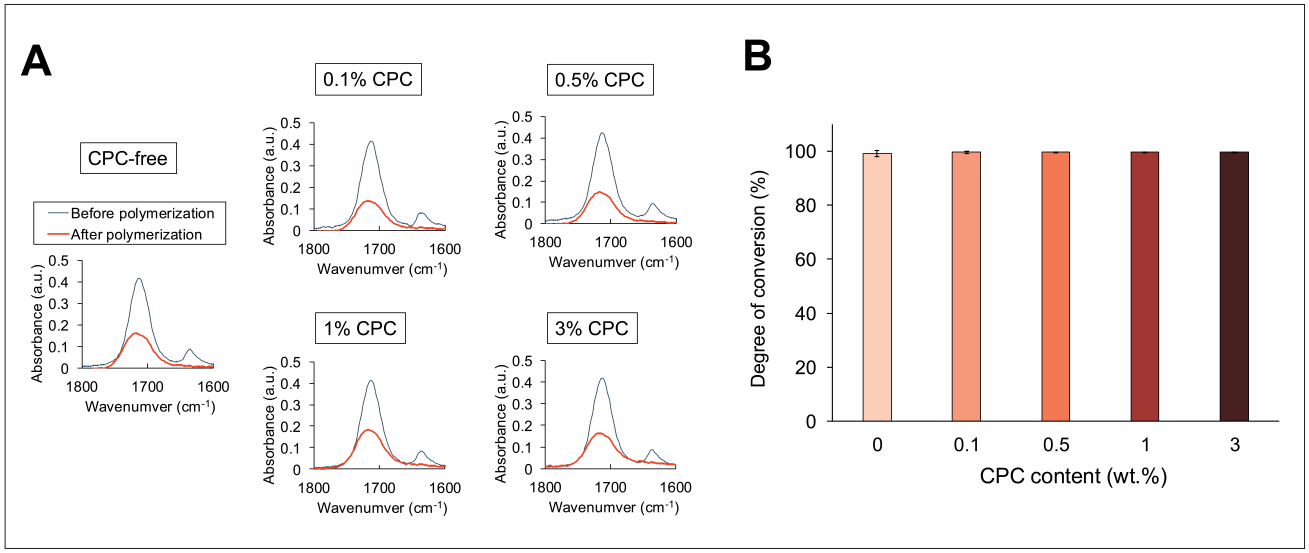

Figure 3. Degree of conversion of the printed resins. (A) Representative Fourier-transform infrared (FTIR) spectra of photocurable resins with different cetylpyridinium chloride (CPC) contents and their corresponding printed resins. (B) Degree of conversion determined by FTIR analysis. No significant differences are observed among the groups. This figure confirms that CPC incorporation does not interfere with the photopolymerization efficiency of the vat photopolymerization resin system.

was not affected by CPC incorporation. These findings indicate that CPC addition up to 1% does not adversely affect the mechanical properties of the printed resin, while higher CPC concentrations (e.g., 3%) reduce mechanical performance.

3.3. Microstructural observation

Figure 5 shows optical microscopy images of the printed resins with different CPC contents. No visible aggregates were observed in the CPC-free, 0.1%, 0.5%, or 1% CPC specimens, indicating a homogeneous microstructure. In contrast, the 3% CPC specimen exhibited distinct CPC-rich aggregates dispersed within the resin matrix, suggesting incomplete dissolution and phase separation.

3.4. Antibacterial properties

The antibacterial properties of the printed resins were evaluated by assessing both antibacterial activity and anti-plaque formation. Figure 6 shows the antibacterial activity of the printed resins, determined by quantifying the number of viable bacteria attached to each specimen. The number of surviving bacteria decreased markedly with increasing CPC content. The CPC-free printed resin exhibited approximately 10^7 CFU ($\log_{10}$NB ≈ 7), whereas the 1% CPC-loaded printed resin showed a substantial reduction to approximately 10^2 CFU ($\log_{10}$NB ≈ 2), which was significantly lower than that of the CPC-free printed resin ($p < 0.05$). The antibacterial activity value (R), defined as the logarithmic difference in bacterial counts between control (CPC-free) and CPC-loaded specimens, was 5.6 for 1% CPC and 7.4 for 3% CPC. According to ISO 22196,[29] an R value greater than 2 (corresponding to a 99% reduction compared with the control) indicates that the material possesses antibacterial activity. Therefore, both the 1% and 3% CPC-loaded printed resins demonstrated effective antibacterial performance.

Figure 7 shows the plaque formation rates, reflecting the sustained antibacterial effect of the 1% CPC-loaded printed resin. Figure 7A presents photographs of plaque-stained specimens. It is evident that the CPC-loaded printed resin exhibited visibly less staining than the CPC-free printed resin, even after the CPC release treatment. These plaque-stained images were further analyzed using image analysis to obtain quantitative values of plaque formation rates, as shown in Figure 7B. Before CPC release, a significant difference was observed between the CPC-loaded (14.6 ± 7.1%) and CPC-free (77.2 ± 20.9%) specimens. After CPC release, the plaque formation rates remained lower for the CPC-loaded specimens (22.7 ± 14.0%) than for the CPC-free samples (88.4 ± 18.1%), and the significant difference persisted ($p < 0.05$). These results indicate that the 1% CPC-loaded printed resin retained its anti-plaque formation activity even after CPC release, demonstrating sustained antimicrobial effectiveness.

3.5. Cetylpyridinium chloride-releasing ability

The CPC-releasing ability of the printed resins was evaluated by UV–Vis spectroscopy (Figure 8). Figure 8A shows the UV–Vis absorption spectra of CPC aqueous solutions with known concentrations used to establish the calibration curve. A characteristic absorption peak was observed at

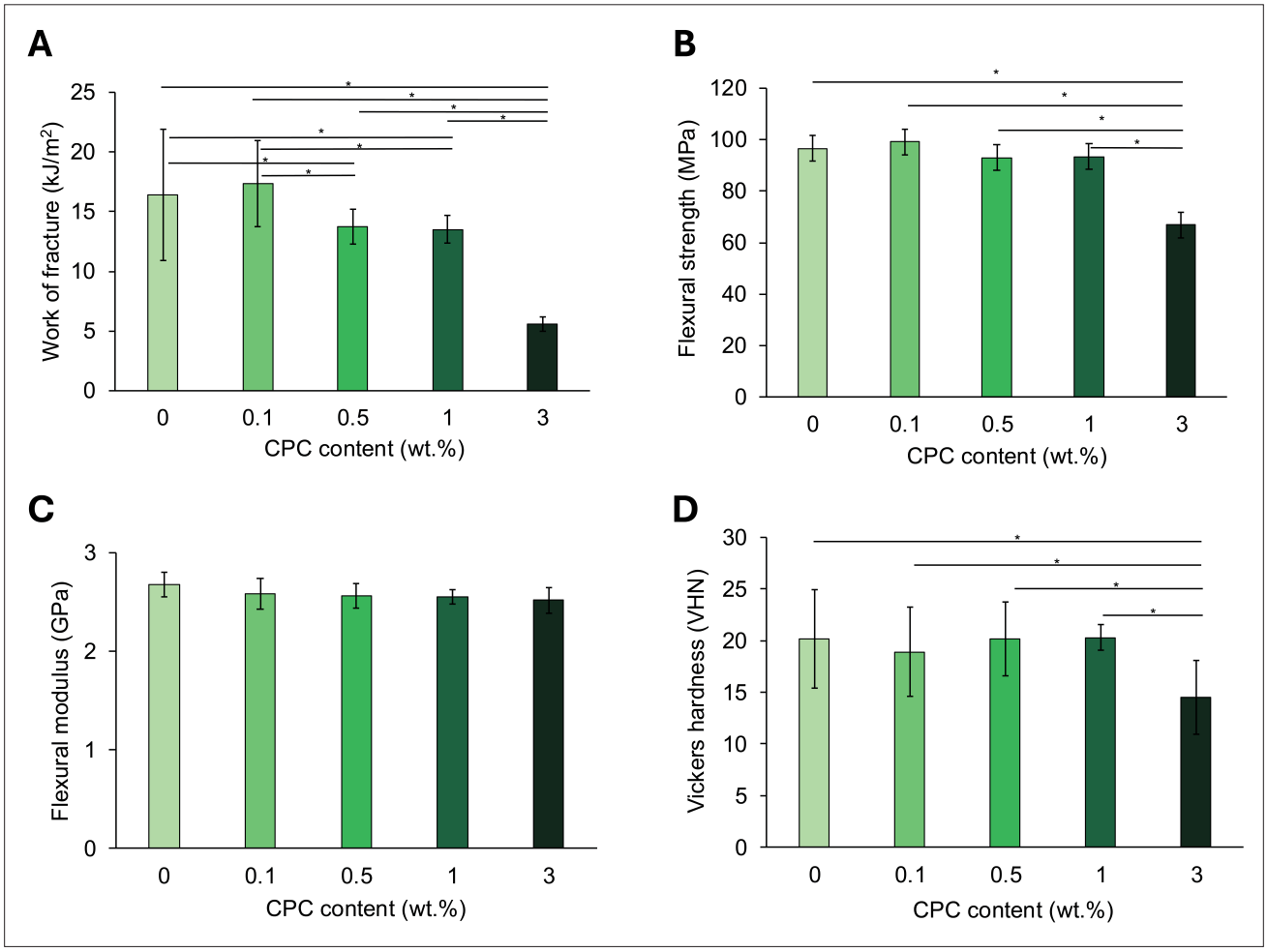

Figure 4. Mechanical properties of cetylpyridinium chloride (CPC)-loaded printed resins with varying CPC contents. (A) Work of fracture. (B) Flexural strength. (C) Flexural modulus. (D) Vickers hardness. The results show that CPC incorporation up to 1% maintains mechanical properties within the range required for dental polymer-based applications, whereas 3% CPC loading leads to a pronounced reduction in strength and fracture resistance. Note: $^*p < 0.05$.

approximately 260 nm, corresponding to CPC. This peak was used to quantify CPC concentrations in the immersion solutions of CPC-loaded printed resins, as shown in Figure 8B. Sustained CPC release was confirmed for specimens containing ≥0.5% CPC. The CPC concentration in the immersion medium gradually increased over time, indicating sustained CPC release from the printed resins throughout the 14-day test period. An initial release was observed at day 1, followed by a continued increase at days 7 and 14. For the 3% and 0.5% CPC-loaded printed resins, the CPC concentrations showed significant differences among the examined time points ($p < 0.05$), confirming sustained release throughout the observation period. A similar increasing trend was observed for the 1% CPC-loaded printed resin; however, the differences among time points were not statistically significant, suggesting a slower and more gradual release profile. In contrast, CPC release from the 0.1% CPC-loaded printed resin remained below the detection limit of the UV–Vis measurement under the present experimental conditions.

To evaluate the cumulative CPC release relative to the total CPC content in the resin, the amount of CPC released into the immersion medium after 14 days was estimated. Approximately 3.5% of the total CPC content was released from the 3% CPC-loaded printed resin, 2.6% from the 1% CPC-loaded printed resin, and 3.5% from the 0.5% CPC-loaded printed resin. These results indicate sustained CPC release without rapid depletion over the experimental period.

4. Discussion

This study aimed to develop a novel CPC-loaded photocurable resin for VPP 3D printing and to evaluate the

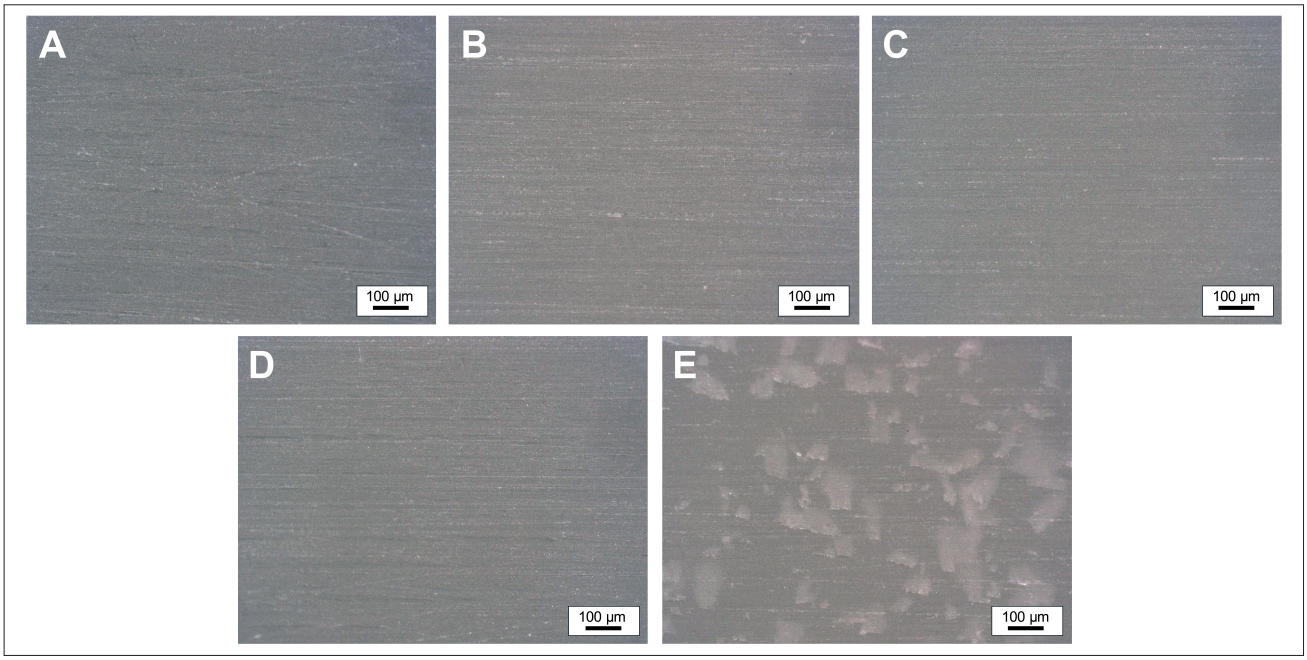

Figure 5. Microscope images of surfaces of the cetylpyridinium chloride (CPC)-loaded printed resins: (A) CPC-free, (B) 0.1% CPC, (C) 0.5% CPC, (D) 1% CPC, and (E) 3% CPC-loaded resins. Scale bars: 100 μm; magnifications: × 300. No visible CPC aggregates are observed in the resin matrices of the CPC-free, 0.1%, 0.5%, and 1% CPC-loaded resins. In contrast, distinct CPC aggregates are observed in the resin matrix of the 3% CPC-loaded resin, indicating incomplete dissolution and phase separation.

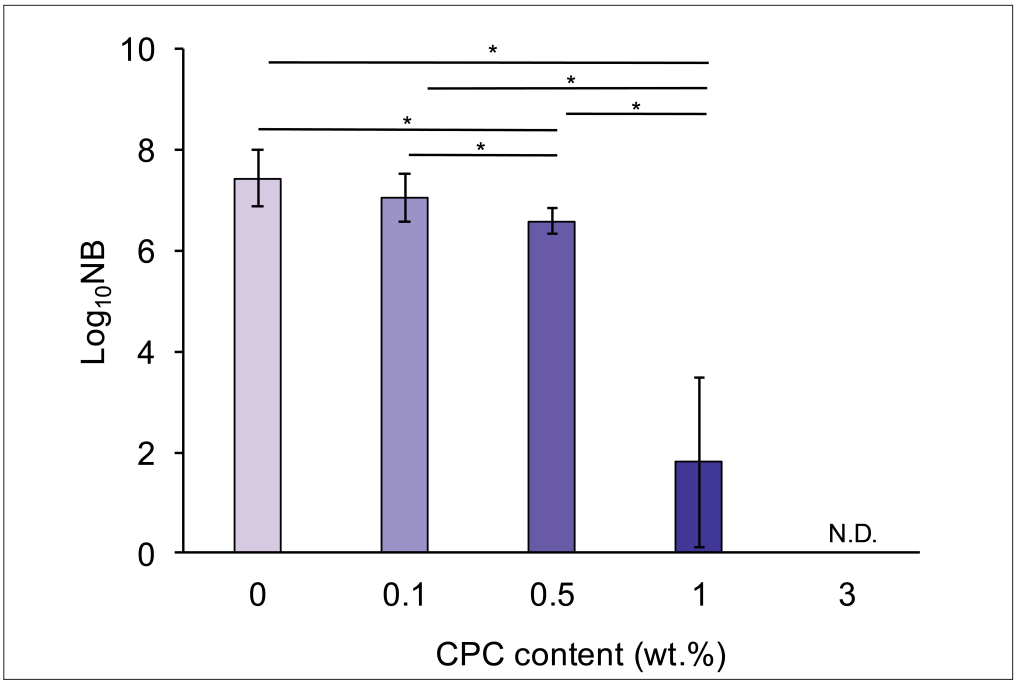

Figure 6. Antibacterial activity of CPC-loaded printed resins against *Streptococcus mutans*. Antibacterial activity was assessed based on bacterial viability, with antibacterial activity values (R) of 0.4 (63.0% reduction) for 0.1% CPC, 0.8 (90.6% reduction) for 0.5% CPC, 5.6 (> 99.99% reduction) for 1% CPC, and 7.4 (> 99.9999% reduction) for 3% CPC. This result indicates that 1% CPC-loading provides strong antibacterial activity exceeding the international performance criterion ($R \geq 2.0$), indicating its effectiveness for antibacterial dental applications. Note: $^*p < 0.05$. Abbreviations: NB, number of bacteria; N.D., not detected; CPC, cetylpyridinium chloride.

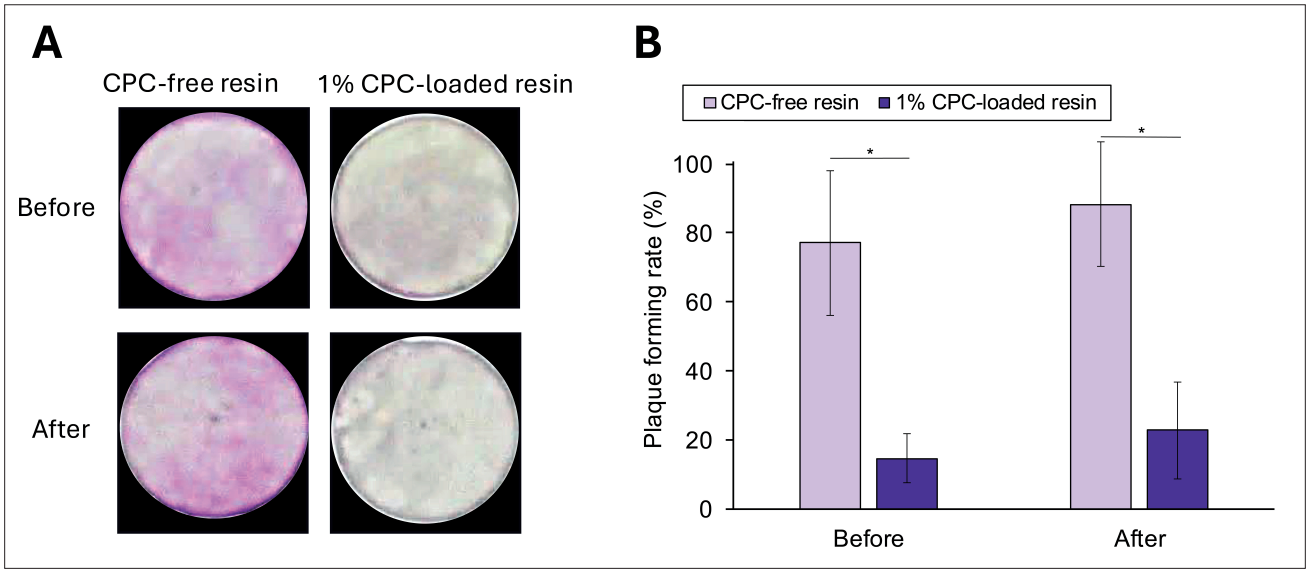

Figure 7. Anti-plaque formation on 1% cetylpyridinium chloride (CPC)-loaded and CPC-free printed resins. (A) Representative images of plaque-stained specimens (diameter: 10 mm) before and after CPC-release treatment by water immersion for 14 days. (B) Quantitative plaque formation rates obtained from the image analysis. These results indicate that the antibacterial effect of the CPC-loaded printed resin is sustained even after prolonged water immersion, suggesting continuous plaque-inhibition capability. Note: $*p < 0.05$.

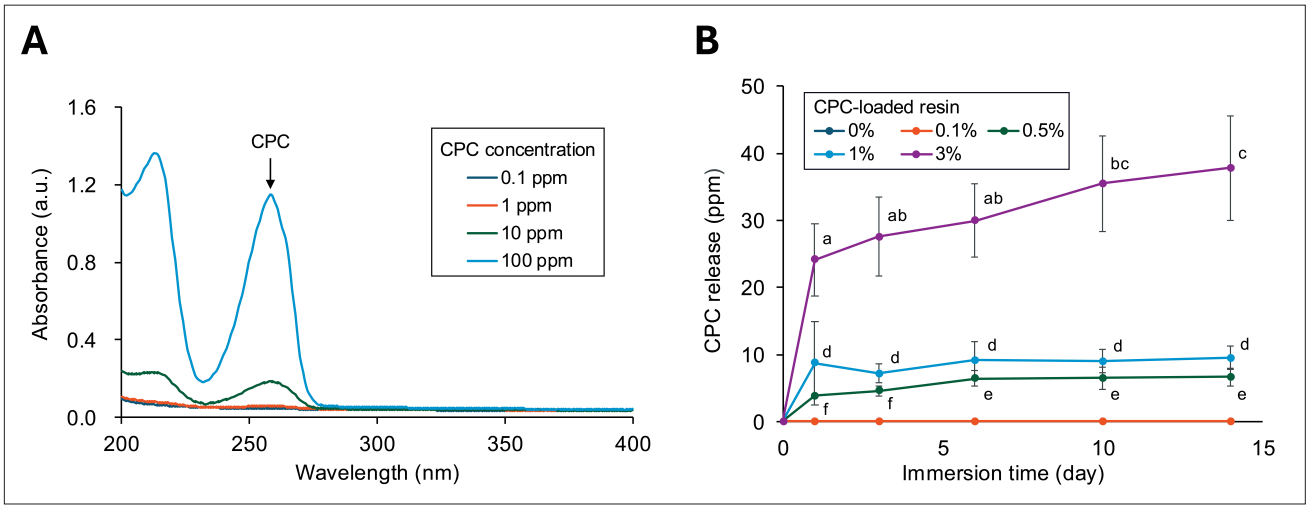

Figure 8. Cetylpyridinium chloride (CPC)-release behavior of CPC-loaded printed resins. (A) Representative UV-Vis spectra of standard aqueous CPC solutions. (B) CPC release profiles of CPC-loaded printed resins immersed in distilled water at 37°C, as determined by UV–Vis spectroscopy. These results confirm sustained CPC release from the printed resins over time, supporting the mechanism underlying their long-term antibacterial activity. Notes: Different letters indicate significant differences among groups at each time point ($p < 0.05$); Statistical analysis was performed within each CPC concentration, comparing CPC release amounts at different time points (days 1, 3, 7, 10, and 14). Different letters indicate significant differences among groups at each time point ($p < 0.05$).

effects of CPC incorporation on printability, mechanical properties, and antibacterial performance of the printed resins. The results demonstrated that the addition of CPC effectively imparted antibacterial activity when incorporated at concentrations of ≥1%, while maintaining acceptable printability and mechanical properties at 1%. These findings indicate that 1% CPC loading enables an optimal balance between antimicrobial function and material performance for the 3D-printed dental resins.

The photocurable resin formulation used consisted of urethane dimethacrylate (UDMA), triethyleneglycol dimethacrylate (TEGDMA), trimethylolpropane triacrylate (TMPTA), and HEMA as base monomers, all of which are commonly employed in dental polymer systems.[30]

In this formulation, each monomer played a distinct and essential role in achieving suitable performance for VPP 3D printing in dental applications. UDMA functioned as the primary backbone monomer, providing mechanical strength to the printed resin. TEGDMA served as a reactive diluent, reducing the viscosity of the photocurable resin and improving its flow behavior to ensure smooth recoating and layer formation during VPP 3D printing. TMPTA, an acrylate monomer with a high density of C=C functional groups, contributed to rapid polymerization and a high crosslink density under the relatively low-intensity light irradiation conditions of the LCD-type VPP printers. HEMA, a hydrophilic monomer containing hydroxyl groups, was critical for dissolving CPC uniformly within the resin matrix.[18] Our preliminary experiments revealed that CPC concentrations above 4% could not be completely solubilized in the monomer mixture, leading to apparent phase separation and compromised printability (data not shown). Therefore, the maximum CPC loading was limited to 3%.

In VPP 3D printing, the printability of resin-based materials is strongly influenced by parameters such as viscosity,[31] cure depth,[32] over-curing behavior,[33] and the photopolymerization characteristics of the resin.[34] Low-viscosity resins can readily flow and fill the narrow gap between the printed object and the vat, ensuring uniform layer formation during the printing process. Conversely, high-viscosity resins exhibit poor flowability, which can prevent complete filling of the gap between the object and the vat, leading to printing defects and poor surface accuracy. The optimal viscosity range for photocurable resins used in VPP printing is generally below 3000 mPa·s.[28] In the present study, the viscosity of all photocurable resins remained below 1000 mPa·s, well within the acceptable range for stable printing.

The cure depth of the photocurable resin is a key factor influencing the continuous stacking of layer-by-layer structures in the 3D printing process. In general, VPP 3D printing employs layer thicknesses of 10–50 μm to achieve high-precision fabrication. Therefore, continuous printing requires the cure depth of the resin to be sufficiently greater than the designated layer thickness to ensure complete interlayer polymerization.[35] The present photocurable resins exhibited a cure depth exceeding 60 μm, which was considered adequate for the continuous curing process required in VPP 3D printing.

Over-curing is an important factor that affects the dimensional accuracy of printed objects. During the light exposure process in VPP 3D printing, part of the irradiated light penetrates or scatters within the resin. Such light penetration and scattering can induce polymerization beyond the intended exposure area, resulting in undesirable over-curing.[36] This phenomenon leads to the overgrowth of the printed object and consequently reduces dimensional accuracy. In the present system, the photocurable resins exhibited increasing degrees of over-curing with higher CPC content, resulting in lateral overgrowth and reduced hole diameters. This phenomenon may be partially attributed to changes in the optical properties of the photocurable resin induced by CPC incorporation. CPC has been reported to exhibit a relatively high refractive index (estimated $n \approx 1.6$),[37] whereas typical methacrylate-based monomers such as UDMA show lower refractive indices (≈1.48).[30] Such a refractive index mismatch may enhance internal light scattering during photoirradiation, potentially contributing to increased over-curing. However, this interpretation should be regarded as a hypothesis, and further optical characterization—such as direct refractive index measurement or light scattering analysis—will be required to clarify the underlying mechanism. For further optimization of resin printability, the over-curing induced by CPC incorporation may be mitigated by adjusting the concentrations of photo-absorbers and photo-initiators, as well as by optimizing light exposure parameters such as irradiation time. Systematic optimization of these factors will be necessary to further improve dimensional accuracy in CPC-loaded resins.

The high degree of conversion observed in the printed resins can be attributed to the highly reactive monomer composition and the intensive post-curing procedure performed under a nitrogen atmosphere. It should be noted that the degree of conversion values, obtained by FTIR analysis, represent relative conversion levels and may approach high values under optimized curing conditions. CPC addition had no significant influence on the degree of conversion. However, increasing CPC content led to a reduction in the mechanical properties of the printed resins, including flexural strength, work of fracture, and Vickers hardness. In particular, the 3% CPC-loaded printed resin exhibited a marked decrease in these properties. This deterioration can be attributed to the non-polymerizable nature of CPC, which lacks reactive functional groups, such as C=C bonds, and therefore cannot be incorporated into the crosslinked polymer network. As shown in Figure 5, while the 1% CPC-loaded printed resin exhibited a homogeneous microstructure, the 3% CPC-loaded printed resin showed visible CPC aggregates, indicating incomplete dissolution and phase separation within the resin matrix. This aggregation potentially acted as a stress concentrator and disrupted the polymer network continuity, thereby contributing to the observed reduction in mechanical properties at 3% CPC loading. Similar reductions in mechanical performance have been reported in the CPC-

loaded methacrylate-based resins when excessive CPC is incorporated.[22,23] In contrast, the 1% CPC-loaded printed resin maintained adequate mechanical properties, meeting the requirements specified in ISO 20795-1:2013 for denture base polymers[38] and ISO 20795-2:2013 for orthodontic base polymers.[39] According to ISO 20795-1:2013, denture base polymers are required to exhibit a minimum flexural strength of 65 MPa and a flexural modulus of 2.0 GPa, whereas ISO 20795-2:2013 specifies minimum values of 50 MPa for flexural strength and 1.5 GPa for flexural modulus for orthodontic base polymers. In the present study, the 1% CPC-loaded printed resin exceeded all of these threshold values, thereby satisfying the mechanical requirements of both ISO standards. These findings suggest that the 1% CPC-loaded printed resin has potential applicability for removable dental prostheses such as dentures, orthodontic aligners, and retainers.

Regarding antibacterial activity, 1% CPC loading effectively inhibited *S. mutans* growth, yielding an *R*-value of 5.6—corresponding to more than 99.99% bacterial reduction—and surpassing the international antibacterial performance criterion ($R \geq 2.0$, 99% reduction).[29] CPC is a well-known cationic surfactant that electrostatically binds to the negatively charged *S. mutans* cell surface and adsorbs onto the cytoplasmic membrane. Its hydrophobic alkyl chain subsequently penetrates the lipid bilayer, resulting in membrane destabilization, increased permeability, and leakage of intracellular components. These events disrupt cellular energy metabolism and ultimately lead to bacterial death. Furthermore, CPC modifies bacterial surface characteristics and suppresses adhesion and biofilm formation. These mechanisms are consistent with the present antibacterial test results. The antibacterial effect observed in this study originated from the sustained release of CPC from the resin matrix, as demonstrated by the 14-day release profile. This gradual release is expected to provide prolonged antibacterial activity, indicating the potential for sustained plaque inhibition in intraoral environments.

To the best of our knowledge, this is the first study to develop a VPP 3D printing resin with intrinsic antibacterial functionality through CPC incorporation. CPC has been widely incorporated into conventional dental resin systems, including poly(methyl methacrylate)-based resins, adhesive materials, and restorative materials, where its antimicrobial efficacy has been well documented. However, these systems differ fundamentally from photocurable resins used in VPP 3D printing, which require precise control of rheological properties, photopolymerization behavior, cure depth, and dimensional accuracy during layer-by-layer fabrication. To date, the incorporation of CPC into VPP-compatible photocurable resin systems has not been systematically investigated. Although CPC was selected due to its established safety and efficacy in oral care products, future research may explore not only CPC but also other biocompatible antibacterial agents—such as isopropyl methylphenol and naturally derived antimicrobials—that may offer enhanced suitability for intraoral applications.[40] Additionally, alternative incorporation strategies, including microencapsulation and covalent immobilization, should be investigated to improve long-term stability and sustained antibacterial performance without compromising the printability or mechanical properties of the resin. The CPC-loaded VPP-printed resin developed in this study also requires further investigation regarding its potential for rechargeable antibacterial functionality, which could enhance its long-term clinical utility. Removable dental prostheses—such as dentures, aligners, and retainers—are routinely cleaned using aqueous cleaning solutions that often contain antimicrobial agents. This daily cleaning process may serve a dual purpose: not only removing accumulated biofilm but also replenishing the CPC content within the resin matrix. Kitagawa *et al.*[18] previously demonstrated that CPC-loaded poly(HEMA/TMPTA) resins were capable of releasing CPC and subsequently being recharged through immersion in CPC-containing solutions. Applying this concept to CPC-loaded VPP-printed resins could enable day-to-day recharging and prolonged antibacterial efficacy. Therefore, future studies should evaluate the CPC recharging capability of VPP-printed materials to establish their long-term antimicrobial performance in clinical use.

Despite the promising results, several limitations of the present study should be acknowledged. First, the photocurable resin formulation contains HEMA, which is known to increase hydrophilicity and water sorption in polymer networks. Increased water uptake may adversely affect dimensional stability and mechanical durability over time, particularly under long-term intraoral conditions. Second, the mechanical properties evaluated in this study represent initial values obtained after printing and post-curing. Long-term mechanical durability under aging conditions—such as prolonged water immersion, thermal cycling, or repeated mechanical loading—was not investigated and should be addressed in future studies to better predict clinical longevity. Third, with respect to biocompatibility, CPC has a well-established safety profile in oral-care products; however, the biocompatibility and cytotoxicity evaluations of CPC-loaded printed resins were not conducted in this study. Therefore, further *in vitro* and *in vivo* assessments will be required to determine the optimal CPC concentration that achieves effective antimicrobial activity without inducing adverse biological effects. Fourth, with respect to antibacterial activity, although the present

study demonstrated antibacterial activity against *S. mutans in vitro*, the oral cavity harbors a complex multispecies biofilm environment.[41] CPC has been reported to exhibit broad-spectrum antimicrobial activity against various oral microorganisms, including *C. albicans* and *Actinomyces* species; however, its penetration into mature biofilms is limited, whereas suppression of initial bacterial adhesion may indirectly inhibit early biofilm development.[21] To verify clinical applicability, future investigations should include antimicrobial assessments against multiple oral microorganisms, as well as *in vivo* evaluations of biofilm formation and plaque inhibition. Ultimately, such comprehensive studies—including preclinical and *in vivo* clinical investigations—will be essential not only for establishing CPC-loaded printed resins as clinically viable materials for antibacterial dental applications but also for validating their intraoral performance and clinical utility.

5. Conclusion

This study demonstrated that CPC can be effectively incorporated into VPP 3D-printed photocurable resins. CPC loading up to 1 wt.% maintained adequate printability. The 1% CPC-loaded printed resin exhibited comparable mechanical properties to the CPC-free printed resin while showing strong antibacterial activity and sustained CPC release. These results indicate that 1% CPC-loading provides an optimal balance among printability, mechanical performance, and antibacterial functionality for 3D-printed dental applications. This study was limited to *in vitro* evaluations using a single bacterial species and a short-term assessment of CPC release; therefore, further investigations are required to validate long-term antibacterial performance under clinically relevant oral conditions.

Acknowledgments

None

Funding

This work was supported by JSPS KAKENHI (grant number 25K20440).

Conflict of interest

The authors declare no conflicts of interest.

Author contributions

Conceptualization: Tomoe Nishikawa, Hiroshi Ikeda
Formal analysis: Jun J. Miyamoto
Funding acquisition: Yusaku Nishizawa, Yasuhiko Akama, Tatsuo Kawamoto
Investigation: Tomoe Nishikawa, Yuki Nagamatsu, Yasuhiko Akama, Yusaku Nishizawa
Methodology: Tomoe Nishikawa, Yusaku Nishizawa, Hiroshi Ikeda
Project administration: Hiroshi Ikeda
Supervision: Tatsuo Kawamoto, Hiroshi Ikeda
Validation: Jun J. Miyamoto, Kaori Gunjigake-Kometani
Writing–original draft: Tomoe Nishikawa, Yuki Nagamatsu, Hiroshi Ikeda
Writing–review & editing: Kaori Gunjigake-Kometani, Tatsuo Kawamoto

Ethics approval and consent to participate

Not applicable.

Consent for publication

Not applicable.

Availability of data

The data that support the findings of this study are available from the corresponding author upon reasonable request.

References

1. Caussin E, Moussally C, Le Goff S, *et al*. Vat photopolymerization 3D printing in dentistry: a comprehensive review of actual popular technologies. *Materials*. 2024;17(4):950. doi: 10.3390/ma17040950

2. Andjela L, Abdurahmanovich VM, Vladimirovna SN, Mikhailovna GI, Yurievich DD, Alekseevna MY. A review on vat photopolymerization 3D-printing processes for dental application. *Dent Mater*. 2022;38(11):e284-e296. doi: 10.1016/j.dental.2022.09.005

3. Jungbauer R, Sabbagh H, Janjic Rankovic M, Becker K. 3D printed orthodontic aligners—a scoping review. *Appl Sci*. 2024;14(22):10084. doi: 10.3390/app142210084

4. Turanoglu OF, Talay Cevlik E, Vural C. Investigation of adhesion status of *Candida* species to the surface of resin materials produced at different angles with additive manufacturing. *BMC Oral Health*. 2024;24(1):738. doi: 10.1186/s12903-024-04505-1

5. Ozer NE, Sahin Z, Yikici C, Duyan S, Kilicarslan MA. Bacterial adhesion to composite resins produced by additive and subtractive manufacturing. *Odontology*. 2024;112(2):460-471. doi: 10.1007/s10266-023-00862-5

6. Tseng CF, Sung CC, Yang YT, *et al*. Impacts of surface characteristics on biological responses and biofilm formation of 3D-printed denture base resins: an in vitro study. *J Dent Sci*. 2025;20(3):1716-1722.

doi: 10.1016/j.jds.2025.03.027

7. Ghezzi B, Artesani L, Giovati L, *et al*. Biological behavior of human gingival fibroblasts and formation of microbial biofilm on 3D-printed dental resin restorations. *Dent Mater*. 2025;41(10):1266-1276. doi: 10.1016/j.dental.2025.07.012

8. Meirowitz A, Rahmanov A, Shlomo E, Zelikman H, Dolev E, Sterer N. Effect of denture base fabrication technique on *Candida albicans* adhesion in vitro. *Materials*. 2021;14(1):221. doi: 10.3390/ma14010221

9. Zalega M, Bociong K. Antibacterial agents used in modifications of dental resin composites: a systematic review. *Appl Sci*. 2024;14(9):3710. doi: 10.3390/app14093710

10. Melo MAS, Garcia IM, Alluhaidan T, *et al*. The next frontier in antibacterial dental resins: a 20-year journey of innovation and expectations. *Dent Mater*. 2025;41(9):1045-1057. doi: 10.1016/j.dental.2025.06.013

11. Salgado H, Gomes A, Duarte AS, *et al*. Antimicrobial activity of a 3D-printed polymethylmethacrylate dental resin enhanced with graphene. *Biomedicines*. 2022;10(10):2607. doi: 10.3390/biomedicines10102607

12. Mangal U, Min YJ, Seo JY, *et al*. Changes in tribological and antibacterial properties of poly(methyl methacrylate)-based 3D-printed intra-oral appliances by incorporating nanodiamonds. *J Mech Behav Biomed Mater*. 2020;110:103992. doi: 10.1016/j.jmbbm.2020.103992

13. Jin G, Ravichandran V, Shim MS, Kim JE. Incorporating an artificially synthesized fluoride complex into urethane-acrylate-based 3D printing resin: effects on mechanical properties, cytotoxicity, antimicrobial actions, and its long-term fluoride-releasing properties. *J Dent*. 2024;150:105363. doi: 10.1016/j.jdent.2024.105363

14. Khattar A, Alghafli JA, Muheef MA, *et al*. Antibiofilm activity of 3D-printed nanocomposite resin: impact of ZrO_2 nanoparticles. *Nanomaterials*. 2023;13(3):591. doi: 10.3390/nano13030591

15. Mao X, Auer DL, Buchalla W, *et al*. Cetylpyridinium chloride: mechanism of action, antimicrobial efficacy in biofilms, and potential risks of resistance. *Antimicrob Agents Chemother*. 2020;64(8):166-191. doi: 10.1128/AAC.00576-20

16. Nezu T, Nagano-Takebe F, Endo K. Designing an antibacterial acrylic resin using the cosolvent method—effect of ethanol on the optical and mechanical properties of a cold-cure acrylic resin. *Dent Mater J*. 2017;36(5):662-668. doi: 10.4012/dmj.2016-222

17. Namba N, Yoshida Y, Nagaoka N, *et al*. Antibacterial effect of bactericide immobilized in resin matrix. *Dent Mater*. 2009;25(4):424-30. doi: 10.1016/j.dental.2008.08.012

18. Kitagawa H, Takeda K, Kitagawa R, *et al*. Development of sustained antimicrobial-release systems using poly(2-hydroxyethyl methacrylate)/trimethylolpropane trimethacrylate hydrogels. *Acta Biomater*. 2014;10(10):4285-95. doi: 10.1016/j.actbio.2014.06.016

19. Matsuo K, Yoshihara K, Nagaoka N, *et al*. Rechargeable antimicrobial adhesive formulation containing cetylpyridinium chloride montmorillonite. *Acta Biomater*. 2019;100:388-397. doi: 10.1016/j.actbio.2019.09.045

20. Kitagawa H, Kitagawa R, Tsuboi R, *et al*. Development of endodontic sealers containing antimicrobial-loaded polymer particles with long-term antibacterial effects. *Dent Mater*. 2021;37(8):1248-1259. doi: 10.1016/j.dental.2021.04.008

21. Otsubo S, Nakanishi K, Fukukawa K, *et al*. Development of autopolymerizing resin material with antimicrobial properties using montmorillonite and nanoporous silica. *Pharmaceutics*. 2023;15(2):544. doi: 10.3390/pharmaceutics15020544

22. Yoshihara K, Nagaoka N, Makita Y, Yoshida Y, Van Meerbeek B. Long-term antibacterial efficacy of cetylpyridinium chloride-montmorillonite containing PMMA resin cement. *Nanomaterials*. 2023;13(9):1495. doi: 10.3390/nano13091495

23. Khan S, Amin F, Amin R, Kumar N. Exploring the effect of cetylpyridinium chloride addition on the antibacterial activity and surface hardness of resin-based dental composites. *Polymers*. 2024;16(5):588. doi: 10.3390/polym16050588

24. Okazaki Y, Nakamori K, Yao C, *et al*. Antibacterial dental adhesive containing cetylpyridinium chloride montmorillonite. *Materials*. 2024;17(17):4368. doi: 10.3390/ma17174368

25. Yoshihara K, Kameyama T, Nagaoka N, *et al*. Development of an antimicrobial coating film for denture lining materials. *Pharmaceutics*. 2025;17(7):902. doi: 10.3390/pharmaceutics17070902

26. Yamamoto Y, Yoshihara K, Nagaoka N, Van Meerbeek B, Yoshida Y. Novel composite cement containing the antimicrobial compound CPC-montmorillonite. *Dent Mater*. 2022;38(1):33-43. doi: 10.1016/j.dental.2021.10.009

27. Perea-Lowery L, Gibreel M, Garoushi S, Vallittu P, Lassila L. Evaluation of flexible three-dimensionally printed occlusal splint materials: an in vitro study. *Dent Mater*. 2023;39(10):957-963. doi: 10.1016/j.dental.2023.08.178

28. Simunovic L, Brenko L, Maric AJ, Mestrovic S, Haramina T. Rheology of dental photopolymers for SLA/DLP/MSLA 3D printing. *Polymers*. 2025;17(19):2706.

doi: 10.3390/polym17192706

29. *ISO Standard 22196; Measurement of Antibacterial Activity on Plastics and Other Non-porous Surfaces*. Geneva, Switzerland: International Standards Organization; 2011.

30. Pratap B, Gupta RK, Bhardwaj B, Nag M. Resin based restorative dental materials: characteristics and future perspectives. *Jpn Dent Sci Rev*. 2019;55(1):126-138. doi: 10.1016/j.jdsr.2019.09.004

31. Taormina G, Sciancalepore C, Messori M, Bondioli F. 3D printing processes for photocurable polymeric materials: technologies, materials, and future trends. *J Appl Biomater Funct Mater*. 2018;16(3):151-160. doi: 10.1177/2280800018764770

32. Bennett J. Measuring UV Curing parameters of commercial photopolymers used in additive manufacturing. *Addit Manuf*. 2017;18:203-212. doi: 10.1016/j.addma.2017.10.009

33. Kolb C, Lindemann N, Wolter H, Sextl G. 3D-printing of highly translucent ORMOCER®-based resin using light absorber for high dimensional accuracy. *J Appl Polym Sci*. 2020;138(3):e49691. doi: 10.1002/app.49691

34. Khan K, Hussain MI, Tareen AK, Asghar A, Hamza M, Chen Z. Advances in vat photopolymerization 3D printing: multifunctional materials, process innovations, and emerging applications. *Mater Sci Eng R Rep*. 2026;167:101120. doi: 10.1016/j.mser.2025.101120

35. Hofstetter C, Orman S, Baudis S, Stampfl J. Combining cure depth and cure degree, a new way to fully characterize novel photopolymers. *Addit Manuf*. 2018;24:166-172. doi: 10.1016/j.addma.2018.09.025

36. Zakeri S, Vippola M, Levänen E. A comprehensive review of the photopolymerization of ceramic resins used in stereolithography. *Addit Manuf*. 2020;35:101177. doi: 10.1016/j.addma.2020.101177

37. ChemBK. *Cetylpyridinium Chloride*. https://www.chembk.com/en/chem/Cetylpyridinium%20chloride. Accessed September 20, 2025.

38. *ISO 20795-1; Dentistry—Base Polymers Part 1: Denture Base Polymers*. Geneva, Switzerland: International Standards Organization; 2013.

39. *ISO 20795-2; Dentistry—Base Polymers Part 2: Orthodontic Base Polymers*. Geneva, Switzerland: International Standards Organization; 2013.

40. Sakagami H, Tomomura M. Dental application of natural products. *Medicines*. 2018;5(1):21. doi: 10.3390/medicines5010021

41. Mosaddad SA, Tahmasebi E, Yazdanian A, *et al*. Oral microbial biofilms: an update. *Eur J Clin Microbiol Infect Dis*. 2019;38(11):2005-2019. doi: 10.1007/s10096-019-03641-9